Communication

Improved breakdown strength and restrained leakage current of sandwich structure ferroelectric polymers utilizing ultra-thin Al2O3 nanosheets

Yi Zeng *, Hao Pan , Zhong-Hui Shen , Yang Shen , Zhi-Fu Liu

Posted Date: 9 October 2023

doi: 10.20944/preprints202310.0489.v1

Keywords: nanosheet; Al2O3; P(VDF-HFP); breakdown strength; leakage

Communication

Improved Breakdown Strength and Restrained Leakage Current of Sandwich Structure Ferroelectric Polymers Utilizing Ultra-Thin Al_2O_3 Nanosheets

Yi Zeng [1,*], Hao Pan [2], Zhong-Hui Shen [3], Yang Shen [2] and Zhi-Fu Liu [4]

[1] Faculty of Printing Packaging Engineering and Digital Media Technology, Xi'an University of Technology, Xi'an 710048, China
[2] School of Materials Science and Engineering, State Key Lab of New Ceramics and Fine Processing, Tsinghua University, Beijing 100084, China
[3] State Key Laboratory of Advanced Technology for Materials Synthesis and Processing, Center of Smart Materials and Devices, Wuhan University of Technology, Wuhan 430070, China
[4] CAS key Lab. Of Information Functional Materials & Devices, Shanghai Institute of Ceramics, Chinese Academy of Sciences, Shanghai 201899, China
* Correspondence: 3115966576@qq.com (Y.Z.); Tel.: +86-17310838356 (Y.Z.)

Abstract: Flexible capacity applications demands to large energy storage density and high breakdown electric field strength of flexible films. Here, P(VDF-HFP) with ultra-thin Al_2O_3 nanosheets composite films were designed and fabricated through an electrospinning process followed by hot-pressing in sandwich structured. The results show that the insulating ultra-thin Al_2O_3 nanosheets and the sandwich structure can enhance the composites' breakdown strength (by 24.8%) and energy density (by 30.6%) remarkedly to P(VDF-HFP) polymer matrix. An energy storage density of 23.5 J/cm^3 at the ultrahigh breakdown strength of 740kV/mm can be therefore realized. Insulating test and phase-field simulation results reveal that ultra-thin nanosheets insulating buffer layers can reduce the leakage current in composites, thus it effects the electric field spatial distribution to enhance breakdown strength. Our research provides a feasible method to increase the breakdown strength of ferroelectric polymers, which is comparable to those of non-ferroelectric polymers.

Keywords: nanosheet; Al_2O_3; P(VDF-HFP); breakdown strength; leakage

1. Introduction

Low-cost electronic and power systems tend to use dielectric capacitive polymers with light weight, low cost, and high energy storage density [1]. Generally, a dielectric material's energy density (U_e) is determined by their electric displacement (D) upon an applied electric field (E), which can be illustrated as $U_e = \int_{D_{max}}^{0} EdD$. [2] Therefore, Therefore, improve D and E can increased energy density in dielectric capacitive polymers. Moreover, a moderate permittivity is needed to refrain from the early electric displacement saturation at a field much lower than breakdown electric field [1]. Generally, dielectric materials of capacitors can be categorized as inorganics (bulk or film ceramics) and organics (polymer). Inorganics can deliver a relative higher energy efficiency and energy density [3–7]. However, their low breakdown strength and non-flexible properties limited the application field. Organics, on the contrary, represent lower cost and easier fabrication in large scale which make them are more commonly used in commercial applications.

The commercially available polymer film capacitors i.e., biaxially oriented polypropylene (BOPP) as a non-polar polymer，it usually possesses high breakdown strengths over 700 MV/m, but low dielectric constants (under 5 for BOPP), thus it has low energy densities of 1~2 J/cm^3 [8,9]. Contrary to non-polar polymers，polar polymer such as ferroelectric based polymers (e.g., poly (vinylidene difluoride): PVDF) usually have high energy density (> 10). However, ferroelectric polymers' C-F bonds have strong orientation polarization, it causes the low breakdown strength in polymers [10]. To improve the breakdown strength and capacitive energy density, polar polymers are extensively investigated with organic blends [11,12] or inorganic fillers of different dimentions,

[13–15] such as nanoparticles (0D) [16–22], nanofibers, nanorod array (one dimensional, 1D) [23–26] as well as nanoplates and nanosheets (two dimensional, 2D) [27–30].

Inorganic nanofillers' morphology and spatial distribution obviously affect the polymers' breakdown strength [31]. In our previous work, 2D insulating nanosheets can enhance the energy effiency and energy density of polar polymer, in contrast to 0D nanoparticles and 1D nanofibers [28]. 2D insulating nanosheets such as Boron Nitride (BN), clay and ZrO_2 et. al. [28,30,32,33] are usually used in nanocomposites. However, it is rather difficult to obtain few-layer or single layer 2D nanosheets, the complicated processing procedure (such as liquid-phase exfoliation) is limited in practical applications.

Here we demonstrate an ultra-thin 2D insulating material-Al_2O_3 nanosheets, which can be achieved through a simple method with a hydrothermal process, instead of the complicated peeling strategy. It is revealed that the incorporation of the 2D Al_2O_3 nanosheets, combined with structure modulation, can remarkably affect ferroelectric based polymers' electric field spatial distribution. Therefore, remarkable improvements in the breakdown strength and energy density are achieved.

2. Experiment

2.1. Preparation of Samples

Figure 1. shows the preparation process diagram of ultra-thin Al2O3 nanosheets (2D-Al2O3) and P(VDF-HFP)/2D-Al_2O_3 nanocomposites. Firstly, $AlCl_3{\cdot}6H_2O$, NaOH, $NH_3{\cdot}OH$ (China National Chemicals Corp. Ltd.) were separately placed in deionized water to a concentration of 1M solution(A), then the NaOH and $NH_3{\cdot}OH$ mixed solution was dropped slowly into A solution until the pH over 8, and then transferred it to the reactor which with teflon lining. Put the reactor in an oven at 200 ° C for over 10 hours, after the reaction, cooling the reactor naturally, and washed the precipitate with deionized water and ethanol repeatedly, then drying the precipitate, obtaining the ultra-thin Al_2O_3 nanosheets (2D-Al_2O_3) powders.

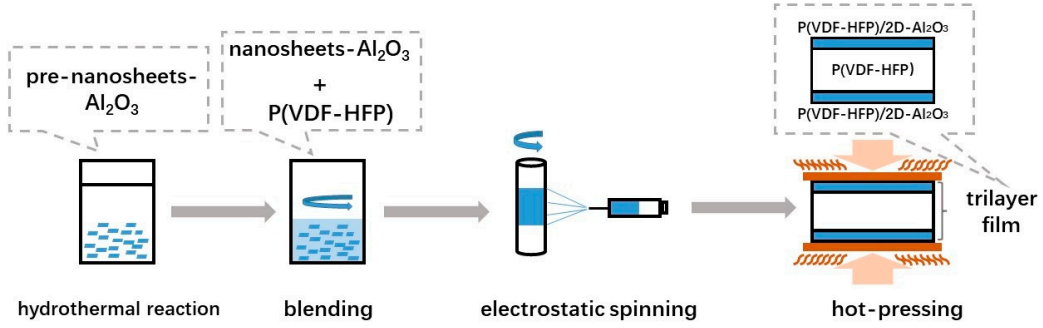

Figure 1. Preparation process diagram of ultra-thin Al_2O_3 nanosheets (2D-Al_2O_3) and P(VDF-HFP)/2D-Al_2O_3 nanocomposites.

Secondly, Al_2O_3 nanosheets powders were dispersed in N,N-dimethylformamide (DMF) and acetone (China National Chemicals Corp. Ltd.). Stirring the mixture over 12h, it makes mixture homogeneous and stable. The Al_2O_3 nanosheets and P(VDF-HFP) (with 10 wt% HFP, Arkema, France, Kynar Flex 2801) are dispersed into N,N-dimethylformamide (DMF), stirring the mixture over 15 h for the homogeneousness, then the precursor sol produced, it is used for the next electrospinning process. The viscosity of the sol is regulated by P(VDF-HFP), then put the sol in injector, electrospinning process is under 1.3 kV cm–1 electric field. After electrospinning, these electrospun fibers are layered by sandwich structure to the next hot-pressing process. The temperature of hot-pressing process is 200°C, 30imn. The last process is reheating the composites to 240°C (for 7 min) and quenching in 0°C water.

A series of sandwich structure in P(VDF-HFP)/ 2D-Al_2O_3 nanocomposites are prepared by the electrospinning process, the trilayered nanocomposites are named as "x0x", "x" is the volume fraction of 2D-Al_2O_3 nanosheets layer, "0" is the pure P(VDF-HFP) layer. For example, "1-0-1" refers to this trilayered films, 1 vol.% 2D-Al_2O_3 nanosheets layers are in the outer layer, and pure P(VDF-HFP) layer is in the middle layer.

2.2. Characterization

Preprints (www.preprints.org) | NOT PEER-REVIEWED | Posted: 9 October 2023 doi:10.20944/preprints202310.0489.v1

The microstructure of Al_2O_3 nanosheets are characterized by an X-ray diffractometer (XRD, D8 Advance) and high-resolution transmission electron microscopy (HRTEM, JEOL2011). The nanocomposites are characterized with scanning electron microscopy (SEM, ZEISS MERLIN compact).

For the measurements of dielectric properties, copper electrodes (2.5 mm in diameter and 50 nm in thickness) are deposited on top of the nanocomposites as the top electrodes, aluminum foil are the bottom electrodes. This research use HP 4990A precision im-pedance analyzer (Agilent) to measure the nanocomposites' dielectric properties at room temperature, the measurement frequency ranges from 10^2 to 10^7 Hz. Using Premier II ferroelectric test system (Radiant Technologies, Inc.) to measure samples' electric displacements–electric field (D–E) loops at 10 Hz. Samples' electric field breakdown strength are measured by Dielectric Withstand Voltage Test (Beijing Elec-tro-Mechanical Research Institute Supesvoltage Technique), current limitation parameter is 5mA, ramping rate is 200V/s.

2.3. Model of Phase-Field [31]

This research use a phase-field model，it's phase-field variable η(r, t) is continuous, this phase-field variable depend on temporally and spatially, therefore, it can be described the P(VDF-HFP)/2D-Al_2O_3 nanocomposites' electrostatic damage process. When phase-field variable is "1", it means the breakdown region, when it is "0", it means non-breakdown region, between these two regions there is transition region，it means the interface region. Because sandwich structure P(VDF-HFP)/2D-Al_2O_3 nanocomposites is a dielectric inhomogeneous system，thus，it's total free energy should be included the electric field，the interface, and the phase separation synergistic contributions，it can be written as

$$F = \int_V \left[f_{sep}(\eta(r)) + \frac{1}{2}\gamma|\nabla\eta(r)|^2 + f_{elec}(r) \right] dV \quad (1)$$

Sandwich structure P(VDF-HFP)/2D-Al_2O_3 nanocomposites' break-down phase evolution process is simulated by A modified Allen–Cahn equation:

$$\frac{\partial\eta(r,t)}{\partial t} = -L_0 H(f_{elec} - f_{critical}) \left[\frac{\partial f_{sep}(\eta)}{\partial\eta(r,t)} - \gamma\nabla^2\eta(r,t) + \frac{\partial f_{elec}(r)}{\partial\eta(r,t)} \right] \quad (2)$$

where L_0 is the kinetic coefficient, it relates to the P(VDF-HFP)/2D-Al_2O_3 nanocomposites' interface mobility. $H(f_{elec} - f_{critical})$ is the Heaviside unit step function ($H(f_{elec} < f_{critical}) = 0$ and $H(f_{elec} > f_{critical}) = 1$). $f_{critical}$ is a material constant which depend on position, it relates to the maximal energy density of each component in the P(VDF-HFP)/2D-Al_2O_3 nanocomposites.

3. Results and Discussion

Polymer matrix with nanofillers usually have an excellent overall performance，therefore，this strategy has been used to improve the composites' energy storage properties. However, the electric field distribution is inhomogeneous in some region, such as it is occurred electric field aggregation in the electric field direction at nanoparticles' shoulders. When the breakdown region come into contact with nanoparticles，it has to detour around the nanoparticles to go forward. Consequently ，the electric field breakdown strength of polymer matrix with nanoparticles is low [31]. For the above reasons, in our previous study, the ferroelectric polymer matrix obtained excellent energy storage performance after switching to nanosheets as an alternative to nanoparticles [28].

Here, our work introduces another nanosheets (2D-Al_2O_3 nanosheets) with a diameter less than 100nm that has ever been reported, are used to replace nanoparticles as the insulating fillers in nanocomposites, meanwhile, study the effect of 2D-Al_2O_3 nanosheets on the electric field distribution in sandwich structure P(VDF-HFP)/2D-Al_2O_3 nanocomposites. Figure 2(a) shows microstructure images of 2D-Al_2O_3 nanosheets with X-Ray Diffraction (XRD) (inner picture) and high-resolution transmission electron microscopy (HRTEM). From Figure 2(a), the nanosheets are well crystallization with a uniform morphology and their crystal size mainly distributes under 100nm.

Trilayered P(VDF-HFP)/2D-Al_2O_3 nanocomposites' microstructure cross section image is shown in Figure 2(b). It shows the homogeneity of P(VDF-HFP)/2D-Al_2O_3 nanocomposites in diffrent layers. Meanwhile, the interface between layers without structure defects, for instance，voids and

Preprints (www.preprints.org) | NOT PEER-REVIEWED | Posted: 9 October 2023 doi:10.20944/preprints202310.0489.v1

pores. The above results means that optimized sandwich structure preparation process has greatly improved the quality of P(VDF-HFP)/2D-Al_2O_3 nanocomposites， thereby it provides a good foundation for improving the properties of dielectric and energy storage.

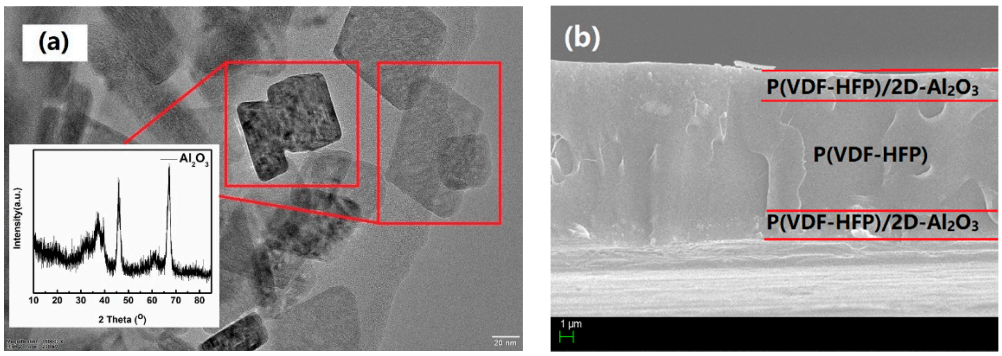

(a) (b)

Figure 2. (**a**) HRTEM and XRD images of 2D-Al_2O_3 nanosheets.; (**b**) Cross-sectional SEM images of P(VDF-HFP)/2D-Al_2O_3 nanocomposites.

Ferroelectric polymer matrix P(VDF-HFP) has a relatively high electric field breakdown strength, while it has a good an open circuit breakdown property. Hence, it has been the dielectrics of potential use for power capacity. And aluminum oxide is a fine favorable insulating material, therefore, it has been commonly used in capacity polymers as a kind of dielectric fillers. To sum up, in this work, sandwich structure P(VDF-HFP)/2D-Al_2O_3 nanocomposites' energy storage properties should be included the electric field，the interface, and the phase separation between the P(VDF-HFP) and aluminum oxide synergistic contributions.

Usually, the energy storage performances are multiply determined by insulating properties, such as capacitances (Figure 3a), the dielectric loss (tanδ) (Figure 3b) and breakdown strength (Figure 4). As shown in Figure 3, the introduction of 2D-Al_2O_3 nanosheets into the ferroelectric polymer matrix can maintain relative high insulating performance, but cannot restrain the dissipation occurring at high frequency, which is mainly caused by resonance of the ferroelectric polymer matrix.

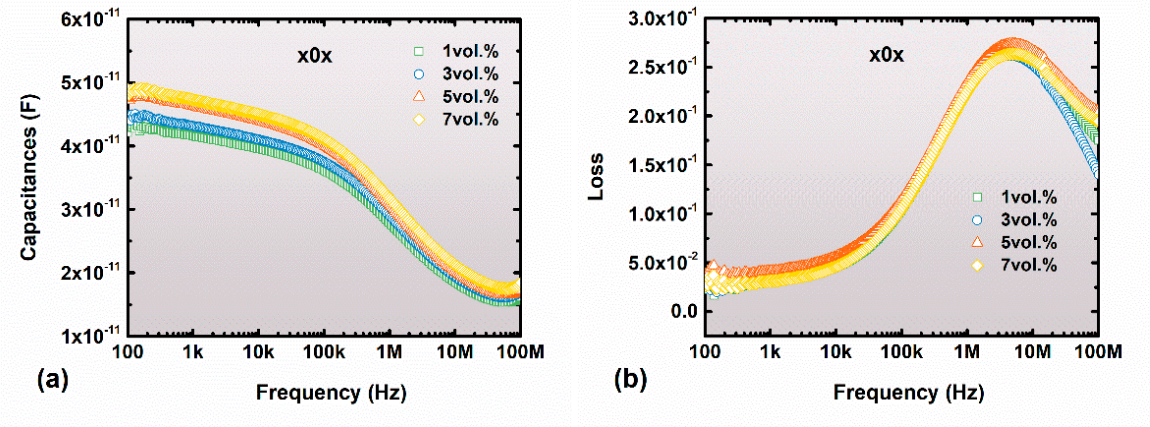

Figure 3. (a)The capacitances and (b)dielectric loss (tan δ) as a function of frequency at 25 °C for the P(VDF-HFP)/2D-Al_2O_3 nanocomposites.

Figure 4 shows the comparison of ferroelectric and energy storage performances between sandwich structure P(VDF-HFP)/2D-Al_2O_3 nanocomposites and P(VDF-HFP) matrix under their breakdown electric fields. However, due to intrinsic electric polarization of P(VDF-HFP), it only bears restricted energy density. In this work, sandwich structure of x0x nanocomposites significantly enhanced electric field strength and electric displacement of ferroelectric polymer matrix. It is calculated that the energy density of x0x nanocomposites is always higher than that of P(VDF-HFP) polymer under the breakdown electric field. The energy density of P(VDF-HFP) is about 18 J/cm^3 at 600kV/mm，while, the energy density of 3-0-3 nanocomposites is about 23.5 J/cm^3 at over 700kV/mm. The higher energy density of 3-0-3 nanocomposites attributes to its higher breakdown strength (E_b).

Preprints (www.preprints.org) | NOT PEER-REVIEWED | Posted: 9 October 2023 doi:10.20944/preprints202310.0489.v1

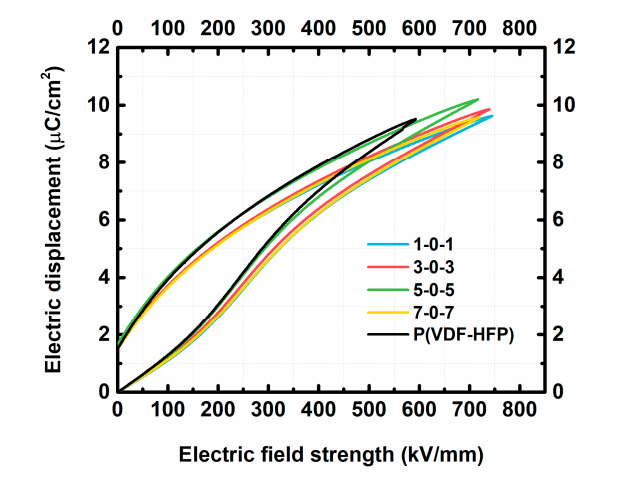

Figure 4. Electric displacement-electric field (D-E) loops of the x0x nanocomposites and P(VDF-HFP) matrix.

For a more detailed comparison between x0x trilayered nanocomposites， P(VDF-HFP) and other references reported ferroelectric composites' energy storage properties, Figure 5 itemizes their discrepancy in the electric field breakdown strength and discharged energy density. Obviously, all of x0x nanocomposites have outstanding properties in the electric field breakdown strength and discharged energy density.

3-0-3 nanocomposite's electric field breakdown strength increased by 24.8% over that of pure P(VDF-HFP) film. The discharged energy density of it is 30.6% higher than that of the pure P(VDF-HFP) film. Both increased breakdown strength and relatively lower energy loss of the x0x nanocomposites cause an increase discharged storage density.

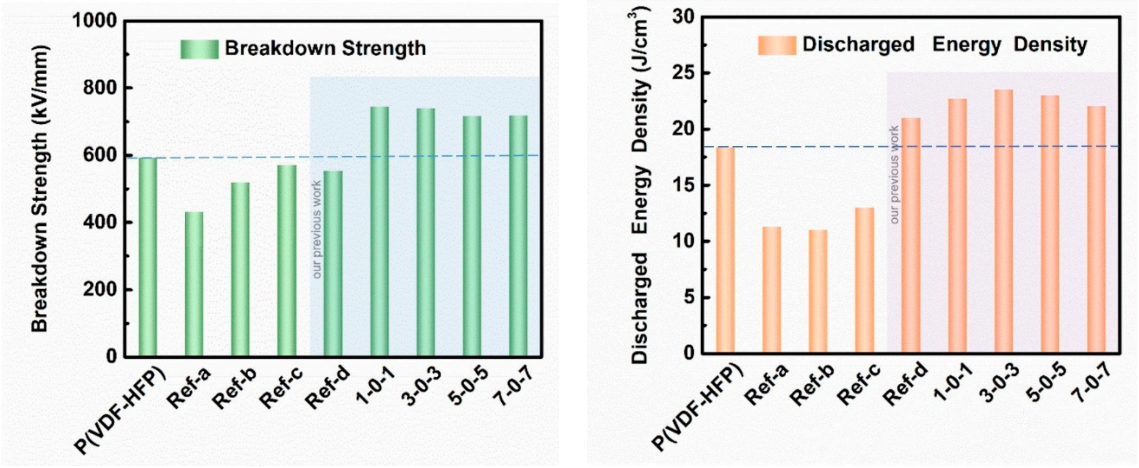

(**a**) (**b**)

Figure 5. Comparisons of (a)breakdown strength and (b)discharged energy density of x0x nanocomposites, P(VDF-HFP) matrix and other nanocomposites. The references in figure 5 are as follows: Ref-a,[17] Ref-b,[34] Ref-c,[29] Ref-d,[28].

To further study which factor affects the efficiency of x0x nanocomposites, we compare the residual polarization values of x0x nanocomposites with field strength in Figure 6. All the nanocomposites have a low remnant displacement of <0.5 μC cm^{-2} until the electric fields increase to 200 kV/mm, because it hasn't had time to get a phase transformation in P(VDF-HFP) before this electric field. It also indicates that the loss is lower when there is low residual polarization at high field strength. When the electric fields rise over 200 kV/cm, field-induced phase transformation occur, the residual polarization values dramatically grow, and it is tending towards stability over 500 kV/cm. It can also be seen from Figure 6 that at 200~500kV/mm, the residual polarization values of 3-0-3 are slightly lower than other samples. This phenomenon is relative to the reduction of ferroelectric

Preprints (www.preprints.org) | NOT PEER-REVIEWED | Posted: 9 October 2023 doi:10.20944/preprints202310.0489.v1

loss, which is corresponding to polymer's decreased loss, when the insulating nanosheets (2D-Al_2O_3) are well-mixed into the polymers.

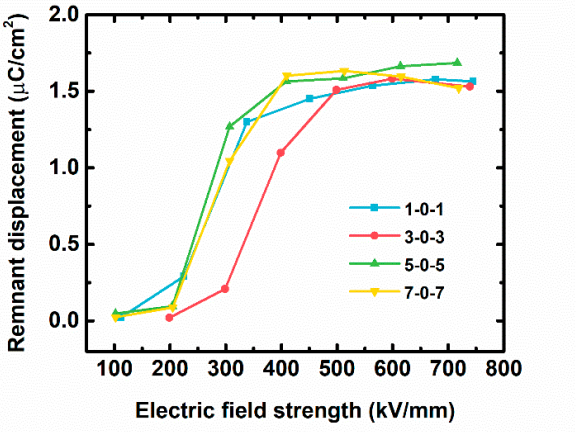

Figure 6. The remnant displacement values of x0x nanocomposites at different electric field strength.

To sum up, the x0x nanocomposites' energy storage density is deeply related to their electric field breakdown strength. Normally, the electric field breakdown strength depends on many parameters, in which electrical tree is one of the main causes. [35,36]. Electrical trees are consisted by many gas channels, these gas channels cause by many factors，for instance，structure defects (voids and pores), partial discharge activity, protrusions from the electrodes, conducting particles and so on [37]. These defects can be suppressed or eliminated by improving the preparation process of nanocomposites. Then, the insulation property is improved to enhanced the energy storage density of x0x nanocomposites.

Here, the x0x structure is designed to restrain the nanocomposites' breakdown effect, which is evidenced by measuring the leakage current at high field strengths (Figure 7). When the field strength is above 200kV/mm, field-induced phase transformation occur, the leakage current of pure P(VDF-HFP) is gradually higher than 2×10^{-6} A/cm². When a small volume ratio of 2D-Al_2O_3 nanosheets are added into pure P(VDF-HFP), a noteworthy feature of x0x nanocomposites is that the leakage current values tend to decrease, which indicates that the good insulation feature of x0x nanocomposites comes from the 2D-Al_2O_3 nanosheets and the sandwich structure synergistic contributions. In previous researches, large contents of dielectric nanoparticles were mixed into polymer matrix aim to increase the polarization or the breakdown strength [38,39]. Nevertheless, nanocomposites' energy storage properties decreased by the large contents of nanoparticles exceeds the permeation threshold [40]. The interesting thing in this work is that when changing the spatial distribution of nanosheets to the interfacial region, the content of nanosheets will be much lower than the percolation threshold while the nanocomposites keep good properties.

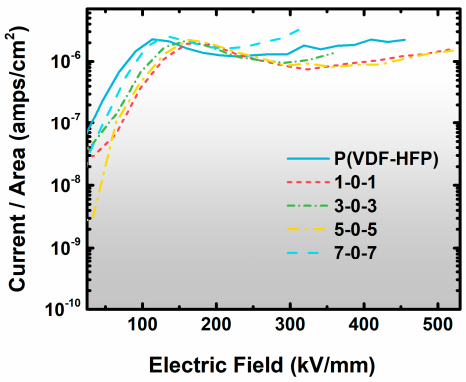

Figure 7. The leakage current of x0x nanocomposites and P(VDF-HFP) matrix at high field strengths.

In addition to test insulating, we also conducted a simulation of the x0x nanocomposites' spatial distribution of the electric field. As shown in Figure 8, it provides deeper understanding about origin of suppressed leakage in nanocomposites. Nanocomposites' microstructure significant impact the

Preprints (www.preprints.org) | NOT PEER-REVIEWED | Posted: 9 October 2023 doi:10.20944/preprints202310.0489.v1

breakdown strength and breakdown path [31]. the charge carriers will have a longer scattering path when they encountering nanosheets, the enhanced electrical performance of nanocomposites is related to those scattered charge and homocharge (which are generated at the electrodes) [41,42]. The function of homocharge is to block the further charge injection，therefore，the voltage is increased [42]. The simulation results revealed that 2D-Al_2O_3 nanosheets are block the flow of electric current between the electrodes. Because of their large isolating interfacial areas that create steric hinderance effect against the growth of electrical trees, the x0x nanocomposite layers near the electrode are acting as buffer layers to bear the electric field. Which leads to not only the high breakdown strengths but also the suppression of leakage current density (i.e., conduction loss) at high fields. These two improvements synergistically contribute to the high energy performance in these nanocomposites.

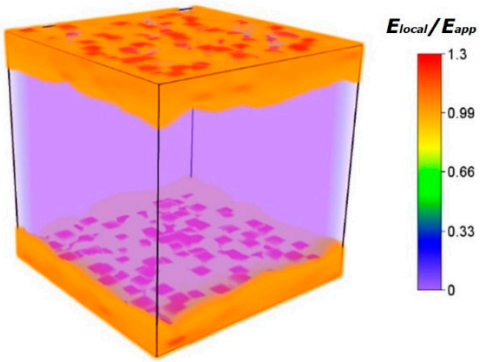

Figure 8. Phase-field simulation of local electric field distribution of P(VDF-HFP)/2D-Al_2O_3 nanocomposite with sandwich structure.

4. Conclusions

In summary, this work demonstrates the feasibility of designing ultra-thin insulating nanosheets and artificial sandwich structures for high-performance dielectric materials. P(VDF-HFP) as a polar polymer with small addition (1-7vol%) of 2D-Al_2O_3 nanosheets as the buffer layers could dramatically increase the electric field breakdown strength by 24.8%, which is about 740kV/mm, while the energy density is improved by 30.6%, which is about 23.5 J/cm^3 in P(VDF-HFP)/2D-Al_2O_3 nanocomposite (with 3 vol.% nanosheets). This work not only proposes new choices for modulating energy storage properties in polar composites but also demonstrates the potential of polar polymer dielectrics to realize high electric breakdown strength comparable to those of non-polar polymers, given that a wide variety of nanosheets are available for nanostructure modulating.

Author Contributions: Conceptualization, Y.Z.; methodology, Y.Z.; software, Z-H.S.; validation, Y.Z. ; data curation, Y.Z. and Z-H.S.; writing—original draft preparation, Y.Z.; writing—review and editing, Y.Z., H.P. and Z-H.S.; supervision, Y.Z., Y.S. and Z-F.L. All authors have read and agreed to the published version of the manuscript.

Funding: This research was funded by Natural Science Basic Research Plan in Shaanxi Province of China, grant number 2020JQ-642; State Key Laboratory of New Ceramic and Fine Processing Tsinghua University, grant number KF201903; the Opening Project of Key Laboratory of Inorganic Functional Materials and Devices, Chinese Academy of Sciences, grant number KLIFM202010.

Data Availability Statement: The data presented in this study are available on request from the corresponding author.

Acknowledgments: The author wishes to express thanks to Professor Yuan-hua Lin, Dr. Jian-Yong Jiang, Dr. Jian-Feng Qian, Dr. ZhenKang Dan, Dr. Meng-Fan Guo, Dr. Tao Zhang, Dr. Zhi-Fang Zhou for their useful help.

Conflicts of Interest: The authors declare no conflict of interest.

References

1. Chu, B. J.; Zhou, X.; Ren, K. L.; Neese, B.; Lin, M. R.; Wang, Q.; Bauer, F.; Zhang, Q. M., A dielectric polymer with high electric energy density and fast discharge speed. Science 2006, 313 (5785), 334-336.
2. Dang, Z. M.; Yuan, J. K.; Yao, S. H.; Liao, R. J., Flexible Nanodielectric Materials with High Permittivity for Power Energy Storage. Adv. Mater. 2013, 25 (44), 6334-6365.
3. Yang, B. B.; Zhang, Q. H.; Huang, H. B.; Pan, H.; Zhu, W. X.; Meng, F. Q.; Lan, S.; Liu, Y. Q.; Wei, B.; Liu, Y. Q.; Yang, L. T.; Gu, L.; Chen, L. Q.; Nan, C. W.; Lin, Y. H., Engineering relaxors by entropy for high energy storage performance. Nature Energy 2023, 13.
4. Li, D.; Zhou, D.; Wang, D.; Zhao, W.; Guo, Y.; Shi, Z.; Zhou, T.; Sun, S.-K.; Singh, C.; Trukhanov, S.; Sombra, A. S. B., Lead-Free Relaxor Ferroelectric Ceramics with Ultrahigh Energy Storage Densities via Polymorphic Polar Nanoregions Design. Small 2023, 19 (8).
5. Pan, H.; Feng, N.; Xu, X.; Li, W. W.; Zhang, Q. H.; Lan, S.; Liu, Y. Q.; Sha, H. Z.; Bi, K.; Xu, B.; Ma, J.; Gu, L.; Yu, R.; Shen, Y.; Wang, X. R.; MacManus-Driscoll, J. L.; Chen, C. L.; Nan, C. W.; Lin, Y. H., Enhanced electric resistivity and dielectric energy storage by vacancy defect complex. Energy Storage Materials 2021, 42, 836-844.
6. Pan, H.; Zeng, Y.; Shen, Y.; Lin, Y.-H.; Ma, J.; Li, L.; Nan, C.-W., $BiFeO_3$-$SrTiO_3$ thin film as a new lead-free relaxor-ferroelectric capacitor with ultrahigh energy storage performance. Journal of Materials Chemistry A 2017, 5 (12), 5920-5926.
7. Pan, H.; Zeng, Y.; Shen, Y.; Lin, Y. H.; Nan, C. W., Thickness-dependent dielectric and energy storage properties of $(Pb_{0.96}La_{0.04})(Zr_{0.98}Ti_{0.02})O_3$ antiferroelectric thin films. J. Appl. Phys. 2016, 119 (12).
8. Rabuffi, M.; Picci, G., Status quo and future prospects for metallized polypropylene energy storage capacitors. IEEE Trans. Plasma Sci. 2002, 30 (5), 1939-1942.
9. Laihonen, S. J.; Gafvert, U.; Schutte, T.; Gedde, U. W., DC breakdown strength of polypropylene films: Area dependence and statistical behavior. IEEE Trans. Dielectr. Electr. Insul. 2007, 14 (2), 275-286.
10. Li, W. J.; Meng, Q. J.; Zheng, Y. S.; Zhang, Z. C.; Xia, W. M.; Xu, Z., Electric energy storage properties of poly(vinylidene fluoride). Appl. Phys. Lett. 2010, 96 (19).
11. Sun, Q.; Shi, B.; Zhang, T.; Yang, W.; Wang, J.; Zhang, L.; Xue, D.; Wang, Z.; Kang, F.; Zhang, X., Dielectric Properties' Synergy of Stretched P(VDF-HFP) and P(VDF-HFP)/PMMA Blends Creates Ultrahigh Capacitive Energy Density in All-Organic Dielectric Films. ACS Applied Energy Materials 2022, 5 (7), 8211-8221.
12. Liu, X.; Luo, H.; Yan, C.; Liu, Y.; Luo, H.; Zhang, D.; Chen, S., Achieving synergistic improvement in dielectric constant and energy storage properties of all-organic liquid crystal molecule/PVDF composites. Journal of Materials Chemistry C 2022, 10 (46), 17757-17767.
13. Behera, R.; K, E., A review on polyvinylidene fluoride polymer based nanocomposites for energy storage applications. Journal of Energy Storage 2022, 48, 103788.
14. Jiang, Y. D.; Zhou, M. J.; Shen, Z. H.; Zhang, X.; Pan, H.; Lin, Y. H., Ferroelectric polymers and their nanocomposites for dielectric energy storage applications. Apl Materials 2021, 9 (2), 11.
15. Zhang, X.; Li, B. W.; Dong, L. J.; Liu, H. X.; Chen, W.; Shen, Y.; Nan, C. W., Superior Energy Storage Performances of Polymer Nanocomposites via Modification of Filler/Polymer Interfaces. Advanced Materials Interfaces 2018, 5 (11), 28.
16. Zhou, W. Y.; Cao, G. Z.; Yuan, M. X.; Zhong, S. L.; Wang, Y. D.; Liu, X. R.; Cao, D.; Peng, W. W.; Liu, J.; Wang, G. H.; Dang, Z. M.; Li, B., Core-Shell Engineering of Conductive Fillers toward Enhanced Dielectric Properties: A Universal Polarization Mechanism in Polymer Conductor Composites. Adv. Mater. 2023, 35 (2), 10.
17. Bi, K.; Bi, M.; Hao, Y.; Luo, W.; Cai, Z.; Wang, X.; Huang, Y., Ultrafine core-shell $BaTiO_3$@SiO_2 structures for nanocomposite capacitors with high energy density. Nano Energy 2018, 51, 513-523.
18. Hu, P. H.; Jia, Z. Y.; Shen, Z. H.; Wang, P.; Liu, X. R., High dielectric constant and energy density induced by the tunable TiO_2 interfacial buffer layer in PVDF nanocomposite contained with core-shell structured TiO_2@$BaTiO_3$ nanoparticles. Appl. Surf. Sci. 2018, 441, 824-831.
19. Hao, Y.; Wang, X.; Bi, K.; Zhang, J.; Huang, Y.; Wu, L.; Zhao, P.; Xu, K.; Lei, M.; Li, L., Significantly enhanced energy storage performance promoted by ultimate sized ferroelectric $BaTiO_3$ fillers in nanocomposite films. Nano Energy 2017, 31, 49-56.

20. Jiang, J.; Zhang, X.; Dan, Z.; Ma, J.; Lin, Y.; Li, M.; Nan, C.-W.; Shen, Y., Tuning Phase Composition of Polymer Nanocomposites toward High Energy Density and High Discharge Efficiency by Nonequilibrium Processing. ACS Appl. Mat. Interfaces 2017, 9 (35), 29717-29731.
21. Chen, G. R.; Wang, X.; Lin, J. Q.; Yang, W. L.; Li, H. D.; Wen, Y. N., Interfacial Polarity Modulation of $KTa_{0.5}Nb_{0.5}O_3$ Nanoparticles and Its Effect on Dielectric Loss and Breakdown Strength of Poly(vinylidene fluoride) Nanocomposites with High Permittivity. J. Phys. Chem. C 2016, 120 (50), 28423-28431.
22. Huang, X. Y.; Xie, L. Y.; Yang, K.; Wu, C.; Jiang, P. K.; Li, S. T.; Wu, S.; Tatsumi, K.; Tanaka, T., Role of Interface in Highly Filled Epoxy/$BaTiO_3$ Nanocomposites. Part II-Effect of Nanoparticle Surface Chemistry on Processing, Thermal Expansion, Energy Storage and Breakdown Strength of the Nanocomposites. IEEE Trans. Dielectr. Electr. Insul. 2014, 21 (2), 480-487.
23. Liu, Y.; Luo, H.; Zhai, D.; Zeng, L.; Xiao, Z.; Hu, Z.; Wang, X.; Zhang, D., Improved Energy Density and Energy Efficiency of Poly(vinylidene difluoride) Nanocomposite Dielectrics Using $0.93Na_{0.5}Bi_{0.5}TiO_3$-$0.07BaTiO_3$ Nanofibers. ACS Appl. Mat. Interfaces 2022, 14 (17), 19376-19387.
24. Zhang, H.; Marwat, M. A.; Xie, B.; Ashtar, M.; Liu, K.; Zhu, Y.; Zhang, L.; Fan, P.; Samart, C.; Ye, Z.-g., Polymer Matrix Nanocomposites with 1D Ceramic Nanofillers for Energy Storage Capacitor Applications. ACS Appl. Mat. Interfaces 2020, 12 (1), 1-37.
25. Pan, Z. B.; Zhai, J. W.; Shen, B., Multilayer hierarchical interfaces with high energy density in polymer nanocomposites composed of $BaTiO_3$@TiO_2@Al_2O_3 nanofibers. Journal of Materials Chemistry A 2017, 5 (29), 15217-15226.
26. Zhang, X.; Shen, Y.; Zhang, Q.; Gu, L.; Hu, Y.; Du, J.; Lin, Y.; Nan, C.-W., Ultrahigh Energy Density of Polymer Nanocomposites Containing $BaTiO_3$ @TiO_2 Nanofibers by Atomic-Scale Interface Engineering. Adv. Mater. 2015, 27 (5), 819-24.
27. Cao, Q.; Zhu, W.; Chen, W.; Chen, X.; Yang, R.; Yang, S.; Zhang, H.; Gui, X.; Chen, J., Nonsolid TiOx Nanoparticles/PVDF Nanocomposite for Improved Energy Storage Performance. ACS Appl. Mat. Interfaces 2022, 14 (6), 8226-8234.
28. Zeng, Y.; Shen, Z. H.; Shen, Y.; Lin, Y. H.; Nan, C. W., High energy density and efficiency achieved in nanocomposite film capacitors via structure modulation Appl. Phys. Lett. 2018, 112 (10), 103902.
29. Zhu, Y. K.; Yao, H.; Jiang, P. K.; Wu, J. D.; Zhu, X.; Huang, X. Y., Two-Dimensional High-k Nanosheets for Dielectric Polymer Nanocomposites with Ultrahigh Discharged Energy Density. J. Phys. Chem. C 2018, 122 (32), 18282-18293.
30. Pan, Z.; Liu, B.; Zhai, J.; Yao, L.; Yang, K.; Shen, B., NaNbO3 Two-Dimensional Platelets Induced Highly Energy Storage Density in Trilayered Architecture Composites. Nano Energy 2017.
31. Shen, Z. H.; Wang, J. J.; Lin, Y. H.; Nan, C. W.; Chen, L. Q.; Shen, Y., High-Throughput Phase-Field Design of High-Energy-Density Polymer Nanocomposites. Adv. Mater. 2018, 30 (2), 6.
32. Shen, Y.; Du, J.; Zhang, X.; Huang, X.; Song, Y.; Wu, H.; Lin, Y.; Li, M.; Nan, C.-W., Enhanced breakdown strength and suppressed leakage current of polyvinylidene fluoride nanocomposites by two-dimensional ZrO_2 nanosheets. Materials Express 2016, 6 (3), 277-282.
33. Ghosh, S. K.; Rahman, W.; Middya, T. R.; Sen, S.; Mandal, D., Improved breakdown strength and electrical energy storage performance of gamma-poly (vinylidene fluoride)/unmodified montmorillonite clay nano-dielectrics. Nanotechnology 2016, 27 (21).
34. He, J.; Yin, Y.; Xu, M.; Wang, P.; Yang, Z.; Yang, Q.; Shi, Z.; Xiong, C., Regenerated Cellulose/$NaNbO_3$ Nanowire Dielectric Composite Films with Superior Discharge Energy Density and Efficiency. ACS Applied Energy Materials 2021, 4 (8), 8150-8157.
35. Budenstein, P. P., On the mechanism of dielectric breakdown of solids. Ieee Transactions on Electrical Insulation 1980, 15 (3), 225-240.
36. Danikas, M. G.; Tanaka, T., Nanocomposites-A Review of Electrical Treeing and Breakdown. IEEE Electr. Insul. Mag. 2009, 25 (4), 19-25.
37. Dissado, L. A.; Fothergill, J. C., Electrical degradation and breakdown in polymers. Peter Peregrinus: 1992; p xix+601.
38. Yu, K.; Niu, Y. J.; Xiang, F.; Zhou, Y. C.; Bai, Y. Y.; Wang, H., Enhanced electric breakdown strength and high energy density of barium titanate filled polymer nanocomposites. J. Appl. Phys. 2013, 114 (17).
39. Li, J. J.; Seok, S. I.; Chu, B. J.; Dogan, F.; Zhang, Q. M.; Wang, Q., Nanocomposites of Ferroelectric Polymers with TiO_2 Nanoparticles Exhibiting Significantly Enhanced Electrical Energy Density. Adv. Mater. 2009, 21 (2), 217-+.

40. McQueen, D. H.; Jager, K. M.; Peliskova, M., Multiple threshold percolation in polymer/filler composites. Journal of Physics D-Applied Physics 2004, 37 (15), 2160-2169.
41. Nelson, J. K. In Overview of nanodielectrics: Insulating materials of the future, 2007 Electrical Insulation Conference and Electrical Manufacturing Expo, 22-24 Oct. 2007; 2007; pp 229-235.
42. Smith, R. C.; Liang, C.; Landry, M.; Nelson, J. K.; Schadler, L. S., The mechanisms leading to the useful electrical properties of polymer nanodielectrics. IEEE Trans. Dielectr. Electr. Insul. 2008, 15 (1), 187-196.